Cancer Chemother Pharmacol (2012) 69:1519–1527
DOI 10.1007/s00280-012-1855-5

ORIGINAL ARTICLE

9-Amino acridine pharmacokinetics, brain distribution, and in vitro/in vivo efficacy against malignant glioma

Aaron M. Teitelbaum · Jose L. Gallardo · Jessica Bedi · Rajan Giri · Adam R. Benoit · Michael R. Olin · Kate M. Morizio · John R. Ohlfest · Rory P. Remmel · David M. Ferguson

Received: 26 August 2011 / Accepted: 15 February 2012 / Published online: 9 March 2012

Abstract
Purpose The delivery of drugs to the brain is a major obstacle in the design and development of useful treatments for malignant glioma. Previous studies by our laboratory have identified a series of 9-amino acridine compounds that block the catalytic cycle of topoisomerase II resulting in apoptosis and cell death in a variety of cancer cell lines.
Methods This study reports the in vitro and in vivo activity of two promising lead compounds, [{9-[2-(1*H*-Indol-3-yl)-ethylamino]-acridin-4-yl}-(4-methyl-piperazin-1-yl)-methanone (**1**) and [9-(1-Benzyl-piperidin-4-ylamino)-acridin-3-yl]-(4-methyl-piperazin-1-yl)-methanone] (**2**), using an orthotopic glioblastoma mouse model. In addition, the absorption, distribution, and metabolism properties are characterized by determining metabolic stability, MDCK accumulation, Pgp efflux transport, plasma protein binding, and brain distribution in mouse pharmacokinetic studies.
Results The efficacy results indicate low micromolar ED_{50} values against glioma cells and a significant increase in the survival of glioma-bearing mice dosed with (**2**) ($p < 0.05$). Pharmacokinetic data collected at time intervals following a 60 mg/kg oral dose of acridine **1** and **2** showed both compounds penetrate the blood–brain barrier yielding peak concentrations of 0.25 μM and 0.6 μM, respectively. Peak plasma concentrations were determined to be 2.25 μM (**1**) and 20.38 μM (**2**). The results were further compared with data collected using a 15 mg/kg intravenous dose of **2** which yielded a peak concentration in the brain of 1.7 μM at 2.0 h relative to a 2.04 μM peak plasma concentration. The bioavailability was calculated to be 83.8%.
Conclusion Taken overall, the results suggest compounds in this series may offer new strategies for the design of chemotherapeutics for treating brain cancers with high oral bioavailability and improved efficacy.

Keywords Acridine · Glioma · Anticancer agents · Pharmacokinetics · In vivo efficacy · Topoisomerase

A. M. Teitelbaum · R. Giri · A. R. Benoit · K. M. Morizio · R. P. Remmel (✉) · D. M. Ferguson (✉)
Department of Medicinal Chemistry, University of Minnesota, Minneapolis, MN, USA
e-mail: remme001@umn.edu

D. M. Ferguson
e-mail: ferguson@umn.edu

J. L. Gallardo · J. Bedi · M. R. Olin · J. R. Ohlfest (✉)
Department of Pediatrics and Neurosurgery, Brain Barriers Research Center, University of Minnesota, Minneapolis, MN, USA
e-mail: ohlfe001@umn.edu

D. M. Ferguson
Center for Drug Design, University of Minnesota, Minneapolis, MN, USA

Introduction

Annually, more than 14,000 people are diagnosed with primary malignant brain cancer in the United States [1]. In addition, less than 5% of patients with glioblastoma, the most devastating and fatal type of brain malignancy, have survived for 5 years following their initial diagnosis [2]. Treatment for glioblastoma with the administration of the DNA alkylating agent temozolomide (Fig. 1), an oral prodrug of MTIC (3-methyl-(triazen-1-yl)imidazole-4-carboxamide), in conjunction with radiotherapy has increased median patient survival to 14.6 months compared with patients receiving radiotherapy alone (12.1 months) [3]. Despite the moderate success of temozolomide treatment, undesirable side effects such as aplastic anemia [4–6], hepatic encephalopathy [7], and most recently urticarial

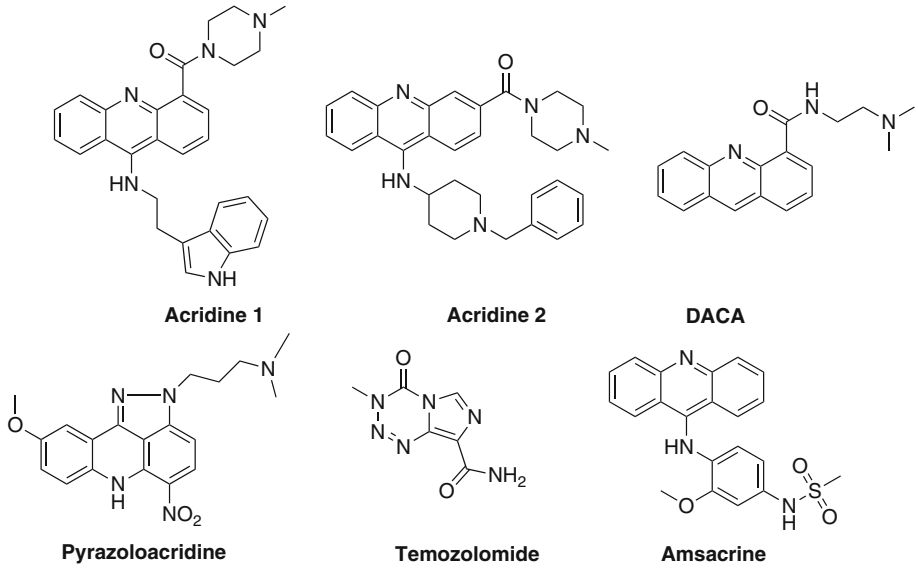

Fig. 1 Chemical structures of acridine **1** and acridine **2**, DACA, pyrazoloacridine, temozolomide, and amsacrine

hypersensitivity [8] have been reported. Several other types of small molecule chemotherapeutic agents for malignant glioma have been investigated only to find a modest increase in patient survival and/or problems with toxicity [9–11]. Clearly, there is still an imperative need for small molecule chemotherapeutics to treat malignant glioma.

Since the 1970s, tricyclic acridine-containing compounds have been investigated as small molecule chemotherapeutic anticancer agents [12, 13]. Mechanisms of action studies have described acridines to be inhibitors of topoisomerase (topo) and telomerase enzymes, which ultimately lead to programmed cell death. Amsacrine (Fig. 1), a characterized "topo poison" and the most successful acridine-based anticancer therapeutic, is clinically used for the treatment of several types of leukemia [14–16]. Cornford and colleagues initially investigated the blood–brain barrier (BBB) permeability of amsacrine and amsacrine derivatives, ultimately confirming that acridine-containing drugs can penetrate the BBB [17]. Interestingly, only two acridine-containing compounds have been used to treat malignant glioma. DACA, N-[2-(dimethylamino)ethyl]-acridine-4-carboxamide (Fig. 1), inhibits both topo I and II by intercalating DNA and stabilizing the cleavable complex between DNA and enzyme. Intraperitoneal administration of DACA to mice resulted in tissue uptake in the brain, liver, kidney, and heart with the greatest accumulation occurring in the liver and kidney [18]. Despite an encouraging low-toxicity profile and high in vitro efficacy, DACA was not further developed due to lack of efficacy in patients with either advanced colorectal cancer, non-small cell lung cancer, advanced ovarian cancer, and glioblastoma multiforme [19–22]. In addition, pyrazoloacridine (PA) (Fig. 1) in combination with platinum-containing compounds has shown encouraging efficacy in T98G glioblastoma cells [23]. However, clinical efficacy was again limited following a PA/carboplatin combination in patients with recurrent glioma [24].

Our research group has recently discovered a series of substituted 9-amino acridines with encouraging anticancer properties that function as topoisomerase II catalytic inhibitors, similarly to aclarubicin [25–27]. To facilitate further clinical development of these compounds, we have characterized their absorption, distribution, and metabolic properties by investigating metabolic stability, permeability, P-glycoprotein (Pgp) and breast cancer resistance protein (BCRP) efflux transport, plasma protein binding, and tissue distribution using mouse pharmacokinetic studies. The pharmacokinetic properties are further applied to select a lead compound for evaluation in an in vivo efficacy study using an orthotopic glioma mouse model. Results are presented that show compound **2** significantly extends the survival of glioma-bearing mice when given once daily in oral doses.

Materials and methods

Chemical materials

Acridine **1** and **2** (Fig. 1) and were synthesized as previously described [25] with purities of 97.8 and 96%, respectively. Tamoxifen was purchased from MP Biomedicals (Solon, OH). Quinidine, Amitriptyline, and Verapamil were all purchased from Sigma-Aldrich (St. Louis, MO). LY335979 trichloride (LY) and GF120918 (GF) were gifts from Dr. Elmquist's laboratory at the University of Minnesota. Solvents and reagents for liquid chromatography included HPLC grade acetonitrile (Sigma-Aldrich, St. Louis, MO), 1-heptane sulfonate sodium salt (Regis Technologies, Morton Grove, IL), and 98% formic acid (Fluka

Analytical, St. Louis, MO). Aqueous reagents were prepared with water purified from a Millipore Elix UV Water Purification System (Millipore, Billerica, MA).

HPLC method development

The HPLC system was composed of an Agilent 1,100 Liquid Chromatograph (Agilent Technologies, Santa Clara, CA), a Phenomenex Gemini C6-Phenyl 100 × 2.0 mm, 5 μm reversed-phase column (Phenomenex, Torrance, CA), and a Shimadzu UV/Vis detector (Shimadzu, Kyoto, Japan) with the wavelength set at 434 nm. Mobile phase A consisted of a 0.05% formic acid aqueous solution containing 5 mM 1-heptane sulfonate, pH 2.8 and mobile phase B was acetonitrile. Acridine **1**, **2**, and a sulfonamide derivative internal standard eluted at 4.06, 5.22, and 6.38 min, respectively, with the following gradient elution: 30% B to 75% B over 8 min with a flow rate of 0.3 mL/min and re-equilibration at 30% for 2.0 min prior to the next injection.

Microsomal stability

Pooled human liver microsomes (HLMs) (BD Biosciencs, San Jose, CA) were incubated at 37°C with acridine **1** or **2** (added in DMSO, final DMSO concentration was <0.1%) for 120 min in the presence of NADPH (EMD Chemicals, Inc., Gibbstown, NJ). The final incubation volume was 0.25 mL and contained the following reagents: 1 μM acridine **1** or **2**, 0.25 mg protein/mL pooled human liver microsomes, 50 mM potassium phosphate buffer, pH 7.4, 1 mM NADPH, and 5 mM $MgCl_2$. All samples were prepared on ice in triplicate, pre-incubated for 2 min at 37°C, followed by the addition of NADPH. Incubations were removed at 5, 10, 15, 30, 45, 60, 90, and 120 min and quenched with 0.25 mL of ice-cold acetonitrile containing the internal standard. Each incubation was added to a 0.2 μM micro-spin filter tube (Chrom Tech, Inc., Apple Valley, MN) and spun at 13,000*g* for 5 min to remove precipitated proteins. The filtrate was then subjected to HPLC-Vis analysis.

Intracellular accumulation in MDCKII cells

Wild-type, MDR1-transfected, and Bcrp1-transfected Madin-Darby canine kidney (MDCKII) cells were kindly provided by Dr. William Elmquist's laboratory at the University of Minnesota. Wild-type cells were cultured in DMEM (Mediatech, Inc., Herndon, VA) supplemented with 10% fetal bovine serum (FBS), penicillin (100 U/mL), and streptomycin (100 μg/mL) (Sigma-Aldrich, St. Louis, MO) and incubated at 37°C and 5% CO_2. MDR1-transfected cells were cultured as described previously but with the addition of colchicine to the media (final concentration 0.22 μM). Bcrp1-transfected cells were cultured with DMEM/F12 media supplemented with FBS and antibiotics. Cultures were passed successively in T-75 tissue culture flasks (Becton–Dickinson, San Jose, CA). Accumulation experiments were performed in 12- or 24-well polystyrene tissue culture plates (Sarstedt, Inc., Newton, NC). All cells were seeded at a density of 2×10^6 cells/well and the media was changed every other day until confluent monolayers were formed. At the start of the experiment, the media were removed from each well by aspiration and the monolayers were washed two times with warmed 37°C cell assay buffer, pH 7.4 (122 mM NaCl, 25 mM $NaHCO_3$, 10 mM glucose, 10 mM HEPES, 3 mM KCl, 1.2 mM $MgSO_4$, 1.4 mM $CaCl_2$, 0.4 mM KH_2PO_4). 1.0 mL of cell assay buffer was added to each monolayer and the plates were pre-incubated at 37°C in an orbital shaker with mild agitation (60 rpm). Subsequently, the media were aspirated and the experiment began by the addition of 1.0 mL of 5 μM acridine **1** or acridine **2** in cell assay buffer. Plates were agitated at 60 rpm and 37°C in an orbital shaker for 120 min. At the end of the 120 min, the drug solutions were immediately aspirated from each well and the wells were washed three times with 1.0 mL ice-cold phosphate-buffered saline. The cells were then lysed by the addition of 0.5 mL 1% Triton X-100 solution. 500 μL of acetonitrile were added to a 500 μL aliquot from each well to precipitate proteins. Samples were spun at 13,000*g* for 2 min and the supernatant was subjected to HPLC-Vis analysis. In addition, the BCA protein assay (Pierce Biotechnology, Inc., Rockford, IL) was utilized to measure protein concentrations in each cell lysate and normalize acridine concentrations from cell monolayers. Acridine concentrations need to be normalized to total protein concentration because the wild-type cells grow at different rates compared with the transfected cells. Acridine accumulation was expressed as the amount of acridine (μmols) per microgram of cellular protein. For the Pgp and BCRP inhibition experiments, cells were treated during both the pre-incubation and incubation times with 1 μM of LY335979 or 5 μM GF120918, respectively. Acridine uptake in the presence of organic cation transporter substrates (70 μM Amitryptiline, 100 μM Verapamil, 100 μM Tamoxifen, 174 μM Quinidine) were also investigated in the wild-type cells.

Plasma protein binding

The binding of Acridine **1** and **2** to human plasma proteins was investigated by an ultracentrifugation technique. Acridine **1** and **2** were added to blank human plasma to achieve a 5 μM concentration. In triplicate, 500 μL of each solution was added to Millipore Centrifree UF Devices (Millipore, Billerica, MA) and centrifuged at 2,000*g* for 30 min. The resulting ultrafiltrate was subjected to HPLC-Vis analysis.

Cell lines

GBM6 and Patient 9 (P-9F) cells were established from surgically dissociated human GBMs at the University of Minnesota. Patient 9-F cells were stably transfected to express a firefly luciferase reporter gene under 2 μg/mL puromycin selection. Cells were maintained as suspended neurospheres in serum-free DMEM/F12 media supplemented with 1% non-essential amino acids, 1% pen/strep, 1X B27, 1X N2, (Invitrogen, Grand Island, NY), and 20 ng/mL EGF and FGF. Cells were incubated in a humidified 37°C atmosphere containing 5% CO_2. Prior to intracranial injection, P9-F neurospheres were centrifuged and dissociated in non-enzymatic cell dissociation buffer (Sigma-Aldrich, St. Louis MO) to form a single-cell suspension. Cell number and viability were determined via trypan blue exclusion on a countess automated cell counter (Invitrogen, Grand Island, NY).

In vitro efficacy

A total of 2,500 GBM6 cells were plated into each well of a 96-well plate, allowed to equilibrate at 37°C and 5% O_2 for 4 h and then were exposed to 100, 33.3, 10, 3.3, and 1 μM of acridine **1** or **2**. Vehicle (phosphate-buffered saline) was administered as a negative control. The cells were incubated for 72 h after which 20 μL MTS (3-(4,5-dimethylthiazol-2-yl)-5-(3-carboxymethoxyphenyl)-2-(4-sulfophenyl)-2H-tetrazolium) (Promega, Madison, WI) was added to each well. Mitochondrial activity was measured using a Synergy/Gen 5 (BioTek, Winooski, VT) plate reader at an absorbance of 490 nm. ED_{50} values were calculated using Microsoft Excel.

Drug formulation and administration

Oral doses of acridine **1** were prepared in a 0.1 M phosphate buffer, pH 3.0 containing 30% polyethylene glycol 200 (Sigma-Aldrich, St. Louis, MO). Oral doses of acridine **2** were prepared in a 0.1 M phosphate buffer, pH 3.0. Each dose contained 1.2 mg acridine/200 μL formulation solution (60 mg/kg) and was administered to the mice by oral gavage. Intravenous doses of acridine **2** were prepared in filter sterilized water containing 40% hydroxypropyl beta-cyclodextrin (Cerestar, Hammond, IN). Each dose contained 0.3 mg acridine/100 μL (15 mg/kg) and was administered via tail vein injection.

Animals

Forty-two female C57BL/6 J mice (stock #: 000664) and 12 female B6.CB17-*Prkdc*^{scid}*/SzJ* mice (stock #: 01913) (Jackson Labs, Bar Harbor, ME) were utilized for the acridine pharmacokinetic investigations and glioma efficacy experiments, respectively. Animals were 6–8 weeks old (20–24 g) at the time of the experiment and were maintained under controlled temperature and humidity while having unlimited access to food and water in a pathogen-free storage facility. The Institutional Animal Care and Use Committee (IACUC) of the University of Minnesota approved all animal procedures.

Sample collection

Single oral and IV dose pharmacokinetic experiments: Following acridine **1** or **2** administration by oral gavage, mice were killed at 1, 2, 4, 8, and 24 h (three mice per time point) by an overdose of ketamine/xylazine. Blood was collected into heparanized vacutainers (BD Biosciences, San Jose, CA) by cardiac puncture. Following aortic perfusion with PBS, the liver, kidney, and brain were excised from the mouse and immediately snap frozen in liquid nitrogen. Acridine **2** was administered via tail vein injection and mice were killed at 0.25, 0.5, 2, 8, 24, and 72 h by an overdose of ketamine/xylazine. Blood and organs were collected as previously described. Plasma was fractionated from whole blood by centrifugation at 2,000 *g*. Each organ was separately weighed in a homogenization test tube and a volume of PBS 3× the organ weight was added. Following homogenization, the tissue homogenates were filtered through gauze to remove any particulates.

Sample preparation

To 0.1 mL of plasma and 0.8 mL of tissue homogenate, were added 0.1 mL and 0.8 mL of methanol containing an acridine sulfonamide internal standard, respectively. The samples were vortexed, refrigerated for 30 min, and centrifuged at 13,000*g* for 10 min. The supernatants were then subjected to the following solid phase extraction (SPE) protocol: C18 Bond Elut (1.0 mL 100 mg) SPE cartridges (Varian, Lake Forest, CA) were conditioned with 1.0 mL 100% methanol and equilibrated with 1.0 mL 0.05% formic acid. 0.1–0.2 mL of plasma and 1.0 mL of tissue homogenate supernatants were loaded onto the cartridge. The cartridges were then washed with 0.5 mL of 30% methanol followed by an additional wash with 70% methanol. Acridines were eluted with 0.5 mL 2% ammonium hydroxide in methanol. Samples were dried under a nitrogen atmosphere at 37°C and reconstituted in 0.1 mL of the HPLC mobile phase.

In vivo efficacy

A total of 50,000 P9-F cells suspended in 1 μL of PBS were injected into the right hemisphere of the brain parenchyma of 6- to 8-week-old female C57BL/6J SCID mice [28, 29].

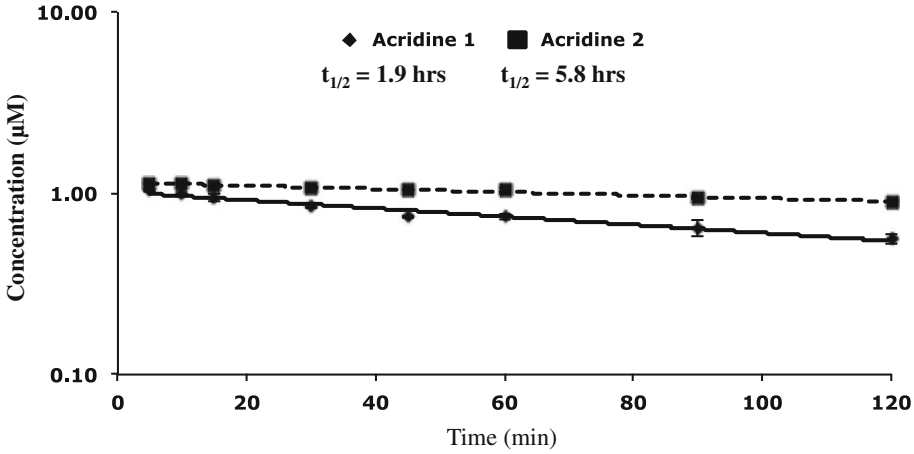

Fig. 2 Oxidative metabolic stability of 1 μM acridine **1** and **2** using pooled human liver microsomes. *Symbols* are the mean ± standard deviation of triplicate samples. *Lines* were fit to a monoexponential equation and half-lives were calculated by dividing the ln 2 by the fractional rate of elimination k_e

Briefly, mice were anesthetized with an IP injection of a cocktail of 54 mg/mL Ketamine and 9.2 mg/mL Xylazine and subsequently placed in a Kopf stereotactic head frame. The scalp was swabbed with betadine and a midline incision was made with a scalpel. A burr hole was placed 2.5 mm lateral and 0.5 mm anterior from sagittal midline located bregma. A Hamilton syringe (26 g) was used to deliver P9-F cells to a 3.3 mm depth from the skull surface to about the middle of the caudate-putamen. Each mouse was randomized and administered a 200 μL dose of acridine **2** via oral gavage on a two-week dosing schedule (days 1–5, 8–12). A 30 mg/kg dose was administered for the first week followed by a 60 mg/kg dose for the second week. Control mice were administered 200 μL of 0.1 M phosphate buffer, pH 3. Mice were closely observed for the duration of the experiment and killed upon any visual morbidity. The Kaplan–Meier curve was generated with GraphPad Prism software.

Pharmacokinetic calculations

The area under the plasma concentration–time curve (AUC) was calculated with the WinNonLin software v5.0.1 (Pharsight, St. Louis, MO). Acridine **2** bioavailability was calculated by the following equation: $F = (\mathrm{AUC_{po}} \times \mathrm{Dose_{iv}})/(\mathrm{AUC_{iv}} \times \mathrm{Dose_{po}})$. Elimination half-life ($t_{1/2}$,) clearance (Cl) and volume of distribution (V_d) were calculated by the following equations: $t_{1/2} = (\ln\ 2/k_e)$ where k_e = fractional rate of elimination, Cl = Dose/AUC, $V_d = \mathrm{Dose}/C_0$ where C_0 is the concentration at time 0.

Statistical analysis

An unpaired Student's *t* test was used to compare the differences of experimental groups. Data are expressed as the mean ± standard deviation. Survival was tested by Log-Rank test. Statistical significance was determined by a $p < 0.05$, indicated by a asterisk.

Results

Metabolic stability

Acridines **1** and **2** (1.0 μM) were incubated in pooled HLMs (0.25 mg protein mL^{-1}), for 120 min in the presence of 1 mM NADPH. Following protein precipitation and HPLC-Vis analysis, no significant metabolites were identified. Half-lives were calculated to be 1.9 and 5.8 h for acridine **1** and **2**, respectively, (Fig. 2). Metabolic stability of acridines **1** and **2** in HLMs supplemented with UDPGA also did not show the formation of any glucuronide metabolites. (Data not shown). The conversion of Flurbiprofen to 4′OH Flurbiprofen was monitored as a positive control.

Intracellular accumulation of acridine **1** and **2**

Acridine **1** and **2** permeability was investigated by comparing their accumulation in MDCK cells with a series of *β*-blockers (atenolol, nadolol, metoprolol, talinolol, and propranolol) which have known permeability. It was found that acridine **1** and **2** similarly accumulate in WT cells with values 2.67 and 2.19 times higher than propranolol, respectively, indicating that acridine **1** and **2** are highly permeable. (Data not shown) Acridine **1** accumulation significantly decreases in both the MDCK-MDR1 (Fig. 3a) and MDCK-Bcrp1 (Fig. 3b) cells, illustrating that acridine **1** is a substrate for both the Pgp and BCRP efflux transporters. In addition, acridine **1** and **2** were thought to be substrates for the organic cation transporter due to the weakly basic nature of acridine-containing compounds. To test this hypothesis, acridine **1** and **2** were incubated in MDCK-WT cells in the presence of various organic cation transporter (OCT) substrates and acridine accumulation was measured (Fig. 3c). Acridine accumulation significantly decreased in the presence of all OCT substrates providing evidence that acridine **1** and **2** are substrates for this transporter.

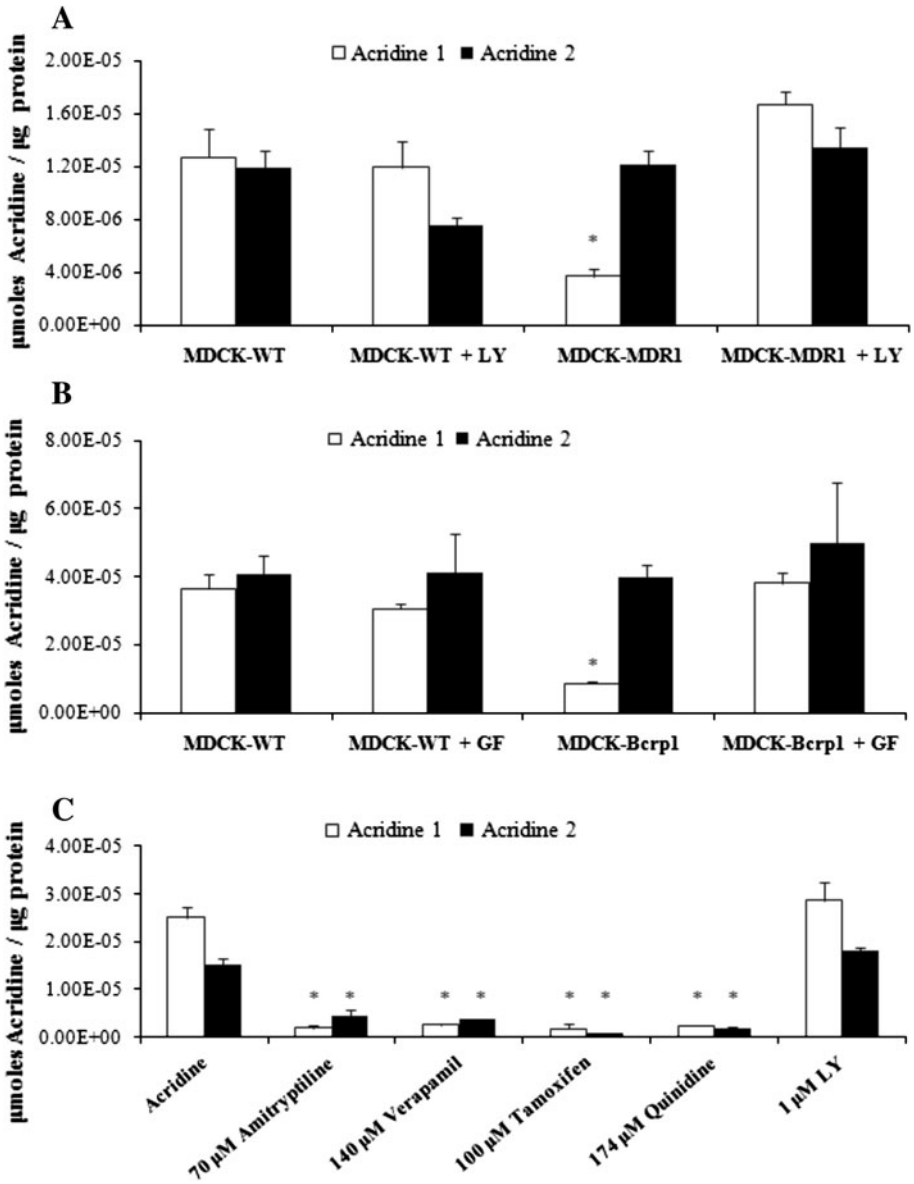

Fig. 3 **a** Acridine **1** and **2** accumulation in MDCK-WT and MDCK-MDR1 transfected cells in the presence of absence of the selective P-glycoprotein (Pgp) inhibitor LY335979 (LY). **b** Accumulation in MDCK-WT and MDCK-Bcrp-1-transfected cells in the presence of absence of the BCRP inhibitor GF120918 (GF). **c** Accumulation in the presence of organic cation transporter substrates Amitryptiline, Verapamil, Tamoxifen, and Quinidine. LY was used as a negative control. The error bars represent the standard deviation of three triplicate samples and significance (*asterisks*) was determined by $p < 0.05$)

In vitro cytotoxicity

The ED_{50} values of acridine **1** and **2** against several human cancer cell lines have been previously described [30]. Efficacy experiments with acridine **1** and **2** against GBM6 cells indicate the lowest ED_{50} values (5.2 and 4.1 µM, respectively) compared with the previously tested cancer cell lines (Table 1).

Plasma protein binding

Protein binding experiments indicated 97.7 and 95.3% binding to human plasma proteins for Acridine 1 and 2, respectively. (Data not shown).

Animal pharmacokinetics

The acridine **1** plasma and brain concentration versus time profiles are presented in Fig. 4a and b. The profiles display a clear mono-exponential decline of acridine 1 indicating a one-compartment model. Following a single 60 mg/kg oral dose of acridine **1**, the C_{max} values of acridine **1** in plasma and brain were 2.25 and 0.2 µM, respectively. The half-life of acridine **1** in plasma and tissue was calculated to be approximately 4.0 h. Fig. 4c depicts the acridine **2** plasma concentration versus time profile in mice that were administered a single oral (60 mg/kg) or IV (15 mg/kg) dose of acridine **2**. These profiles display a two-compartment model with a both distributional and elimination phase. The

Table 1 Acridine **1** and **2** in vitro efficacy against a variety of cancer cell lines

Acridine	1	2
GBM6	5.2 ± 2.8	4.1 ± 1.9
DU145	37.2 ± 12.1	32.4 ± 8.8
HCT-116	29.0 ± 8.7	29.2 ± 4.1
Hepa-1c1c7	55.9 ± 5.3	26.9 ± 6.6
H460	16.0 ± 6.9	38.5 ± 3.6
MCF-7	37.2 ± 6.2	25.7 ± 5.0
SU86.86	6.8 ± 2.2	21.2 ± 5.1
MEL	16.7 ± 4.1	14.6 ± 3.2
OCL-3	39.8 ± 8.6	20.3 ± 4.6
REH	19.7 ± 4.9	21.0 ± 4.5

Cancer cells: GBM6 (glioblastoma), DU-145 (prostate), HCT-116 (colon), Hepa-1c1c (liver), H460 (non-small lung), MCF-7 (breast), SU86.86 (pancreatic), MEL (melanoma), OCL-3 (ovarian), and REH (kidney). Values reported are EC_{50} ± SE (μM)

Table 2 Pharmacokinetic parameters from the oral and IV dose of acridine **2** administered to mice

Administration	Oral	IV
Dose (mg/kg)	60	15
C_{max} (μM)	20.38[a]	2.04[b]
Clearance (L/h)	0.0326[c]	0.0394
AUC_{0-24} (h μmol/L)	61.63	18.37
V_d (L)	N/A	0.266
Free fraction	0.047	
F	86%	

[a] C_{max} at 1.0 h after oral administration

[b] C_{max} at 15 min after IV administration

[c] Apparent oral clearance (Cl/F)

plasma half-life of acridine **2** (22.2 h) was approximately 5 times longer than acridine **1** (4.46 h).

Following the IV dose, a distributional half-life (4.68 h) was calculated instead of a terminal half-life because the concentration at the 72-h time point was below the limit of detection for the assay. Both the volume of distribution (0.266 L) and bioavailability (84%) were high, and due to the long half-life of acridine **2**, clearance was very slow, 0.0394 L/h (Table 2). Figure 4d illustrates the brain concentration of acridine **2** versus time following the oral and IV dose. The brain pharmacokinetics from the oral dose displays unusual pharmacokinetics (concentration decreases and then increase). The C_{max} of acridine **2** in the brain following the single IV dose (1.7 μM) was 2.8 times higher than the brain C_{max} following the oral dose.

In vivo efficacy

Mice-bearing glioma were treated with acridine **2** via oral gavage. Mice were dosed once daily, M–F for two weeks (Fig. 5). During the first week, the mice were treated with

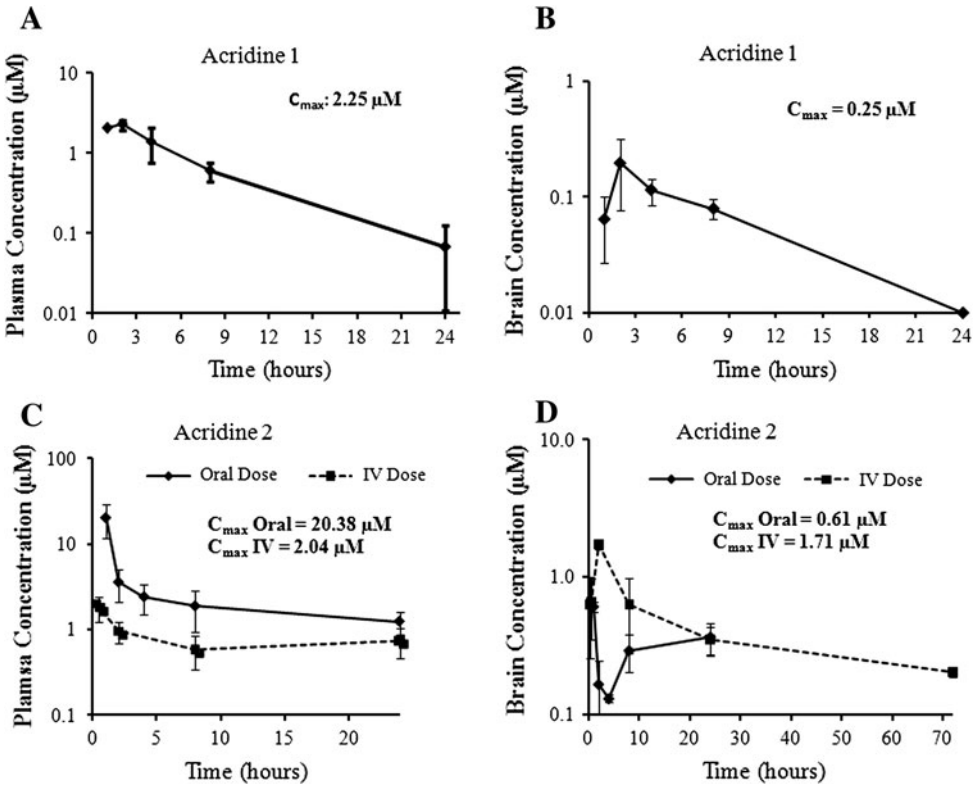

Fig. 4 Acridine **1** and **2** plasma and brain concentration versus time profiles in C57BL-6 female mice. **a**, **b** Plasma and brain log concentrations of acridine **1** versus time in mice treated orally with a single dose of 60 mg/kg acridine **1. c**, **d** Plasma and brain concentration of acrdine **2** versus time in mice treated orally with a single dose (60 mg/kg) and intravenously (15 mg/kg) of acridine **2**. Maximum concentration (C_{max}). *Symbols* are the mean of 3 animals ± standard deviation

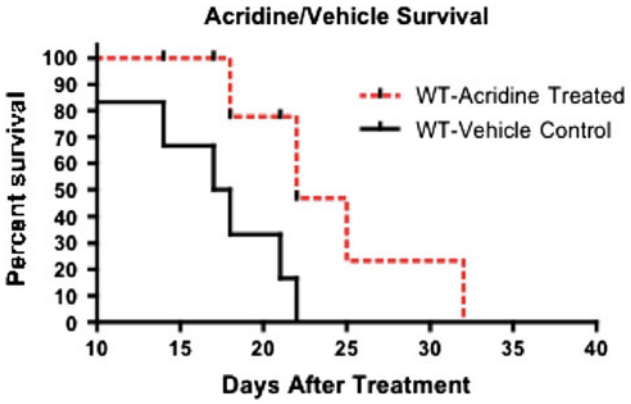

Fig. 5 Kaplan–Meier survival curve of untreated and acridine **2** treated mice. $p < 0.05$ for the survival between treated and untreated animals

30 mg/kg of acridine **2** followed by 60 mg/kg during the second week. All of the untreated mice died within two weeks of glioma implantation; however, there was a significant increase in the survival ($p < 0.0375$) of mice treated with acridine **2**.

Discussion

Our research group has discovered a series of small molecule 9-aminoacridine-based compounds with low micromolar ED_{50} values against human glioma cell lines (Table 1). Permeability and mouse pharmacokinetic studies led us to choose acridine **2** for in vivo efficacy experiments due to its higher brain penetration and limited efflux by Pgp and BCRP compared with acridine **1**. Acridine **2** significantly increased the median survival of mice in an orthotopic glioblastoma model (Fig. 5). To our knowledge, this is the first evidence of in vivo efficacy against malignant glioma from both a topoisomerase II inhibitor and acridine-containing compound. We hypothesize that our compounds gain access to the brain by passive diffusion due to their high lipophilicity: ClogP values of 5.52 and 5.28 for acridine **1** and **2**, respectively. Although DACA and PA were administered to patients with malignant glioma, the BBB permeability was never initially investigated. The CLogP values of DACA and PA are 3.1 and 4.2, respectively, and thus are less lipophilic than acridine **1** and **2**. This may explain the failure of DACA and PA to show efficacy against glioma. Alternatively, they may be better substrates for efflux pumps. Other topoisomerase II inhibitors such as etoposide, doxorubicin, and mitoxantrone are thought to suffer from high efflux (Pgp and BCRP), limiting their application in the clinic [31].

Efflux may also explain the higher concentration achieved in the brain for acridine **2**. In comparing cellular concentrations of compounds **1** and **2** in Pgp and BCRP overexpression systems (Fig. 3), acridine **1** shows lower accumulations indicating it is a more favorable substrate for Pgp and BCRP efflux than acridine **2**. This may be due to the greater positive charge on compound **2**. At physiological pH, the piperidine nitrogen of acridine **2** is more easily ionized than the indole nitrogen of acridine **1** and thus accounts for the greater overall positive charge of acridine **2**. Also, acridine **2** is less bound to human plasma proteins than acridine **1** (95 and 98%, respectively).

Preliminary experiments also have been performed that suggest acridines **1** and **2** are substrates for an organic cation transporter (Fig. 3C). We believe the OCT-2 transporter is the predominant isoform involved in acridine transport because MDCK cells have been previously shown to express OCT-2 specifically with little to no expression of the other isoforms (OCT-1 and OCT-3) [32]. Lin and colleagues recently discovered that both OCT-1 and OCT-2 are expressed on the luminal side of brain microvessel endothelial isolated from humans, mice, and rats [33]. In addition to passive diffusion, acridine **1** and **2** may be entering the brain through the OCT uptake transporters expressed on the luminal membrane of the brain capillary endothelial cells.

One issue that is not addressed here is the difference noted in the plasma and brain concentration versus time profiles of acridine **1** and **2**. While the pharmacokinetics of acridine **1** suggests a one-compartment model, the data observed for acridine **2** are consistent with a two-compartment model. The origin of this disparity is unclear but may be due to transport mechanisms or mouse to mouse variability. Acridine **2** does bear an additional positive charge, which may have a significant impact on distribution and elimination, especially if OCT transport is involved. Nevertheless, the high oral bioavailability of acridine **2** and long half-life is extremely encouraging in the design and development of new agents for treating malignant glioma. Additional experiments are underway to better understand the role OCT plays in mediating transport of these compounds across the blood brain barrier with the ultimate goal of reaching higher, more efficacious concentrations of drug in the brain.

Acknowledgments This research was supported by R01CA138437 (JRO), the Center for Drug Design at the University of Minnesota and the Children's Cancer Research Fund.

References

1. Louis DN, Ohgaki H, Wiestler OD, Cavenee WK, Burger PC, Jouvet A, Scheithauer BW, Kleihues P (2007) The 2007 WHO classification of tumours of the central nervous system. Acta Neuropathol 114(2):97–109
2. CBTRUS (2011) CBTRUS statistical report: primary brain and central nervous system tumors diagnosed in the United States in

2004–2007. http://www.cbtrus.org/2011-NPCR-SEER/WEB-0407-Report-3-3-2011.pdf
3. Stupp R, Mason WP, van den Bent MJ, Weller M, Fisher B, Taphoorn MJ, Belanger K, Brandes AA, Marosi C, Bogdahn U, Curschmann J, Janzer RC, Ludwin SK, Gorlia T, Allgeier A, Lacombe D, Cairncross JG, Eisenhauer E, Mirimanoff RO (2005) Radiotherapy plus concomitant and adjuvant temozolomide for glioblastoma. N Engl J Med 352(10):987–996
4. Jalali R, Singh P, Menon H, Gujral S (2007) Unexpected case of aplastic anemia in a patient with glioblastoma multiforme treated with Temozolomide. J Neurooncol 85(1):105–107
5. George BJ, Eichinger JB, Richard TJ (2009) A rare case of aplastic anemia caused by temozolomide. South Med J 102(9):974–976
6. Kopecky J, Priester P, Slovacek L, Petera J, Kopecky O, Macingova Z (2010) Aplastic anemia as a cause of death in a patient with glioblastoma multiforme treated with temozolomide. Strahlenther Onkol 186(8):452–457
7. Goldbecker A, Tryc AB, Raab P, Worthmann H, Herrmann J, Weissenborn K (2011) Hepatic encephalopathy after treatment with temozolomide. J Neurooncol 103(1):163–166
8. Pothiawala S, Hsu MY, Yang C, Kesari S, Ibrahimi OA (2010) Urticarial hypersensitivity reaction caused by temozolomide. J Drugs Dermatol 9(9):1142–1144
9. Galanis E, Buckner JC (2010) Enzastaurin in the treatment of recurrent glioblastoma: a promise that did not materialize. J Clin Oncol 28(7):1097–1098
10. Neyns B, Sadones J, Chaskis C, Dujardin M, Everaert H, Lv S, Duerinck J, Tynninen O, Nupponen N, Michotte A, De Greve J (2011) Phase II study of sunitinib malate in patients with recurrent high-grade glioma. J Neuro Oncol 103(3):491–501
11. Murray LJ, Bridgewater CH, Levy D (2011) Carboplatin chemotherapy in patients with recurrent high-grade glioma. Clin Oncol 23(1):55–61
12. Denny WA (2002) Acridine derivatives as chemotherapeutic agents. Curr Med Chem 9(18):1655–1665
13. Belmont P, Bosson J, Godet T, Tiano M (2007) Acridine and acridone derivatives, anticancer properties and synthetic methods: where are we now? Anti Cancer Agents Med Chem 7(2):139–169
14. Dekker AW, van't Veer MB, Sizoo W, Haak HL, van der Lelie J, Ossenkoppele G, Huijgens PC, Schouten HC, Sonneveld P, Willemze R, Verdonck LF, van Putten WL, Lowenberg B (1997) Intensive postremission chemotherapy without maintenance therapy in adults with acute lymphoblastic leukemia. Dutch Hemato-Oncology Research Group. J Clin Oncol 15 (2):476–482
15. Mollgard L, Tidefelt U, Sundman-Engberg B, Lofgren C, Lehman S, Paul C (1998) High single dose of mitoxantrone and cytarabine in acute non-lymphocytic leukemia: a pharmacokinetic and clinical study. Ther Drug Monit 20(6):640–645
16. Harousseau JL, Cahn JY, Pignon B, Witz F, Milpied N, Delain M, Lioure B, Lamy T, Desablens B, Guilhot F, Caillot D, Abgrall JF, Francois S, Briere J, Guyotat D, Casassus P, Audhuy B, Tellier Z, Hurteloup P, Herve P (1997) Comparison of autologous bone marrow transplantation and intensive chemotherapy as postremission therapy in adult acute myeloid leukemia. The Groupe Ouest Est Leucemies Aigues Myeloblastiques (GOELAM). Blood 90(8):2978–2986
17. Cornford EM, Young D, Paxton JW (1992) Comparison of the blood-brain barrier and liver penetration of acridine antitumor drugs. Cancer Chemother Pharmacol 29(6):439–444
18. Evans SM, Young D, Robertson IG, Paxton JW (1992) Intraperitoneal administration of the antitumour agent N-[2-(dimethylamino)ethyl]acridine-4-carboxamide in the mouse: bioavailability, pharmacokinetics and toxicity after a single dose. Cancer Chemother Pharmacol 31(1):32–36
19. Caponigro F, Dittrich C, Sorensen JB, Schellens JH, Duffaud F, Paz Ares L, Lacombe D, de Balincourt C, Fumoleau P (2002) Phase II study of XR 5000, an inhibitor of topoisomerases I and II, in advanced colorectal cancer. Eur J Cancer 38(1):70–74
20. Dittrich C, Coudert B, Paz-Ares L, Caponigro F, Salzberg M, Gamucci T, Paoletti X, Hermans C, Lacombe D, Fumoleau P (2003) Phase II study of XR 5000 (DACA), an inhibitor of topoisomerase I and II, administered as a 120-h infusion in patients with non-small cell lung cancer. Eur J Cancer 39(3):330–334
21. Dittrich C, Dieras V, Kerbrat P, Punt C, Sorio R, Caponigro F, Paoletti X, de Balincourt C, Lacombe D, Fumoleau P (2003) Phase II study of XR5000 (DACA), an inhibitor of topoisomerase I and II, administered as a 120-h infusion in patients with advanced ovarian cancer. Invest New Drugs 21(3):347–352
22. Twelves C, Campone M, Coudert B, Van den Bent M, de Jonge M, Dittrich C, Rampling R, Sorio R, Lacombe D, de Balincourt C, Fumoleau P (2002) Phase II study of XR5000 (DACA) administered as a 120-h infusion in patients with recurrent glioblastoma multiforme. Ann Oncol 13(5):777–780
23. Adjei AA, Budihardjo II, Rowinsky EK, Kottke TJ, Svingen PA, Buckwalter CA, Grochow LB, Donehower RC, Kaufmann SH (1997) Cytotoxic synergy between pyrazoloacridine (NSC 366140) and cisplatin in vitro: inhibition of platinum-DNA adduct removal. Clin Cancer Res 3(5):761–770
24. Galanis E, Buckner JC, Maurer MJ, Reid JM, Kuffel MJ, Ames MM, Scheithauer BW, Hammack JE, Pipoly G, Kuross SA (2005) Phase I/II trial of pyrazoloacridine and carboplatin in patients with recurrent glioma: a North Central Cancer Treatment Group trial. Invest New Drugs 23(5):495–503
25. Goodell JR, Madhok AA, Hiasa H, Ferguson DM (2006) Synthesis and evaluation of acridine- and acridone-based anti-herpes agents with topoisomerase activity. Bioorg Med Chem 14(16):5467–5480
26. Goodell JR, Ougolkov AV, Hiasa H, Kaur H, Remmel R, Billadeau DD, Ferguson DM (2008) Acridine-based agents with topoisomerase II activity inhibit pancreatic cancer cell proliferation and induce apoptosis. J Med Chem 51(2):179–182
27. Oppegard LM, Ougolkov AV, Luchini DN, Schoon RA, Goodell JR, Kaur H, Billadeau DD, Ferguson DM, Hiasa H (2009) Novel acridine-based compounds that exhibit an anti-pancreatic cancer activity are catalytic inhibitors of human topoisomerase II. Eur J Pharmacol 602(2–3):223–229
28. Wiesner SM, Freese A, Ohlfest JR (2005) Emerging concepts in glioma biology: implications for clinical protocols and rational treatment strategies. Neurosurg Focus 19(4):E3
29. Olin MR, Andersen BM, Zellmer DM, Grogan PT, Popescu FE, Xiong Z, Forster CL, Seiler C, SantaCruz KS, Chen W, Blazar BR, Ohlfest JR (2010) Superior efficacy of tumor cell vaccines grown in physiologic oxygen. Clin Cancer Res 16 (19):4800–4808
30. Galvez-Peralta M, Hackbarth JS, Flatten KS, Kaufmann SH, Hiasa H, Xing C, Ferguson DM (2009) On the role of topoisomerase I in mediating the cytotoxicity of 9-aminoacridine-based anticancer agents. Bioorg Med Chem Lett 19(15):4459–4462
31. Loscher W, Potschka H (2005) Role of drug efflux transporters in the brain for drug disposition and treatment of brain diseases. Prog Neurobiol 76(1):22–76
32. Shu Y, Bello CL, Mangravite LM, Feng B, Giacomini KM (2001) Functional characteristics and steroid hormone-mediated regulation of an organic cation transporter in Madin-Darby canine kidney cells. J Pharmacol Exp Ther 299(1):392–398
33. Lin CJ, Tai Y, Huang MT, Tsai YF, Hsu HJ, Tzen KY, Liou HH (2010) Cellular localization of the organic cation transporters, OCT1 and OCT2, in brain microvessel endothelial cells and its implication for MPTP transport across the blood-brain barrier and MPTP-induced dopaminergic toxicity in rodents. J Neurochem 114(3):717–727